5. CHETAEV N.G., Stability of Motion. Gostekhizdat, Moscow, 1955.
6. MIL'SHTEIN G.N., Stability and stabilization of periodic motions of autonomous systems, PMM, 41, 1, 1977.
7. STARZHINSKII V.M., Orobital stability in the special case of the three-body problem. Questions of Mechanics. Selected Questions of Dynamics, Coll. of Papers Moscow Soc. of Natural Scientists, Phys. Sec., Nauka, Moscow, 1976.
8. MARKEYEV A.P. and SOKOL'SKII A.G., A method of constructing and investigating the stability of periodic motions of autonomous Hamiltonian systems. PMM, 42, 1, 1978.
9. ZUBOV V.I., Theory of Vibrations. Vyssh. Shkola, Moscow, 1979.
10. SUSLOV G.K., Rotation of a heavy solid around a fixed pole (S.V. Kovalevskaya case), Trudy, Otdel. Fizich. Nauk Obshch. Lyubitelei Estestvoznaniya, 7, 2, 1895.
11. GOLUBEV V.V., Lectures on Integration of the Equations of Motion of a Heavy Solid around a Fixed Point. Gostekhizdat, Moscow, 1953.
12. POZHARITSKII G.K., On the construction of Lyapunov functions from integrals of the perturbed motion equations, PMM, 22, 2, 1958.
13. ROUSH N., ABETS P. and LALUA M., The Direct lyapunov Method in Stability Theory, Mir, Moscow, 1980.
14. RUMYANTSEV V.V., On the stability of motion with respect to part of the variables, Vestnik, Moscow, Gosudarst. Univ., Ser. Matem., Mekhan., As tron., Fiziki, Khimii, 4, 1957.
15. RUMYANTSEV V.V., On the stability of permanent rotations of a solid around a fixed point, PMM, 21, 3, 1957.
16. SAVCHENKO A.YA., Stability of Stationary Motions of Mechanical Systems. Naukova Dumka, Kiev, 1977.

Translated by M.D.F.

PMM U.S.S.R., Vol.50, No.6, pp.753- 762, 1986
Printed in Great Britain

0021-8928/86 $10.00+0.00

ON THE TRANSITION MODE CHARACTERIZING THE TRIGGERING OF A VIBRATOR IN THE SUBSONIC BOUNDARY LAYER ON A PLATE*

O.S. RYZHOV and E.D. TERENT'EV

The problem of the development of two-dimensional linear perturbations in a boundary layer, generated by the triggering of a vibrator, is considered. Fourier transformations in the longitudinal coordinate and a Laplace transform in time are used to construct the solution. The inverse transforms are evaluated for large values of the characteristic time t and all values of the longitudinal coordinate x. Domains located downstream of the vibrator are studied in the first of which the perturbations will have the form of Tollmien-Schlichting waves that go over into a wave packet in the second domain. The identity in the structure of the wave packets, which are orthonormalized to the maximum amplitude for this packet for different frequencies of vibrator oscillation is noted.

Vibrating tapes located either on a streamlined surface or within the stream are often used in experimental installations for investigating boundary layer stability. Measurements are made when the harmonic mode of vibrator operation is built up, the transient that originates when it is triggered is considered to be of slight interest and for this reason is not considered. If the frequency of the forced oscillations exceeds the critical value, the formulation of the appropriate boundary value problem is fraught with serious difficulties since the solution must be sought in a class of functions with exponential growth in the longitudinal coordinate. Conditions which ensure the uniqueness of the solution are spoiled since an exponentially increasing eigenfunction of the homogeneous boundary value problem can be appended with arbitrary weight to any solution. The emergence from the situation created relies on the postulate proposed in /1/ according to which the solution at each fixed time

*Prikl.Matem.Mekhan., 50, 6, 974-986, 1986

and at each given point of space should be a continuous function of the parameters, including the frequency of the forced harmonic perturbations. This postulate ensures uniqueness in the selection of the weighting factor before the eigenfunction.

To provide a foundation or to disprove the postulate being discussed, a solution should be constructed for the more general problem with initial data on the triggering of the vibrator, switched in at a certain time. Such a problem was examined in /2/, where the main attention was concentrated on calculating the pressure for times which increased without limit and for large, but finite, distances along the length of the plate downstream of the source of oscillation. It is shown that for the times and distances under consideration, the perturbations behind the vibrator take the form of monochromatic Tollmien-Schlichting waves with frequency equal to the frequency of the source in conformity with the postulate put forward in /1/.

The flow is studied below in the intermediate domain where connection of the unperturbed boundary layer ahead of it occurs with the Tollmien-Schlichting wave behind it. This domain is occupied by a vortex spot (wave packet) characterizing the triggering of the vibrator. The tongue of the vortex spot moving most rapidly ahead carries information in its structure about the initial stage of the motion of the vibrator brought out from rest, but the amplitude of the gas oscillations is small in this part. The centre of the spot contains pulsations with the highest amplitude, where their nature is determined by the internal properties of the boundary layer with selfinduced pressure. In the real part of the spot, the span of the oscillations again diminishes, here the perturbation field depends on the frequency of the forcing force but this dependence is manifested weakly at subcritical frequencies. A vibrator operating at subcritical frequency in experimental installations can be used to generate laminar vortex spots.

1. Formulation of the problem. Let a uniform subsonic ideal gas stream impinge on a plate with a vibrator on its surface. We select the frequency, longitudinal dimension, and amplitude of the source oscillations such that the motion it excites could be described by the theory of free boundary layer interaction /3-5/. Expressing both the independent variable and the desired functions in units of the special dimensionless system of this theory, we allow the intensity of the perturbations to tend to zero. In the system mentioned t is the time, x and y are Cartesian space coordinates, and u' and v' are the vector components of the velocity pulsations found from the solution of the linearized Prandtl equations

$$\frac{\partial u'}{\partial x}+\frac{\partial v'}{\partial y}=0,\quad \frac{\partial u'}{\partial t}+y\frac{\partial u'}{\partial x}+v'=-\frac{\partial p'}{\partial x}+\frac{\partial^2 u'}{\partial y^2},\quad \frac{\partial p'}{\partial y}=0 \tag{1.1}$$

for an incompressible fluid, where the excess pressure p', unknown in advance, will satisfy the additional limit condition

$$u'\to\frac{1}{\pi}\int\limits_{-\infty}^{x}dx_1\int\limits_{-\infty}^{\infty}\frac{p'(t,x_2)}{x_2-x_1}\,dx_2,\quad y\to\infty \tag{1.2}$$

We assume that the vibrator is triggered at a time $t=0$, therefore, for $t<0$ the stream impinges on a smooth plate $y_w=0$. When $t\geqslant 0$ we consider the moving part of the streamlined surface (membrane) of triangular shape and oscillating sinusoidally; hence

$$y_w=f(x)\sin\omega_0 t \tag{1.3}$$

$$f(x)=\begin{cases}0, & x\leqslant 0 \quad \text{or} \quad x\geqslant a\\ 2x, & 0\leqslant x\leqslant b\\ 2b(a-x)/(a-b), & b\leqslant x\leqslant a\end{cases} \tag{1.4}$$

The frequency ω_0 and the parameters a and b are positive.

Since the initial Blasius boundary layer is unperturbed, the initial condition asserts

$$u'=0,\quad t=0 \tag{1.5}$$

The conditions for gas adhesion to the vibrating membrane are

$$u'=-f(x)\sin\omega_0 t,\quad v'=\omega_0 f(x)\cos\omega_0 t,\quad y=0,\quad t\geqslant 0 \tag{1.6}$$

2. Application of integral transforms. Let us expand the solution of problems (1.1)-(1.6) in Laplace integrals in time and Fourier integrals in the longitudinal coordinate

$$[\bar u(\omega,k,y),\bar v(\omega,k,y),\bar p(\omega,k)]=\int\limits_{-\infty}^{\infty}dx\int\limits_{-\infty}^{\infty}e^{-(\omega t+ikx)}[u'(t,x,y),v'(t,x,y),p'(t,x)]\,dt$$

Substituting them into the Linearized Prandtl equations, we obtain a system of ordinary differential equations for the function-transforms $\bar{u}, \bar{v}$ and $\bar{p}$. Integration of this system is by means of the scheme developed in /6-9/ and relies on the introduction of the complex independent variable

$$z = \Omega + i^{1/3}k^{1/3}y, \quad \Omega = i^{-1/3}\omega k^{-1/3} \tag{2.1}$$

As ever, the main difficulty is in constructing the originals by using the inverse transforms. Of all the transforms under consideration, $\bar{p}$ has the simplest expression because it is independent of the transverse coordinate y. Let $\mathrm{Ai}(z)$ denote the Airey function and let us set

$$F(\Omega, k) = \Phi(\Omega) - Q(k) \tag{2.2}$$

$$\Phi = \frac{d\,\mathrm{Ai}(\Omega)}{dz} I^{-1}(\Omega), \quad I = \int_{\Omega}^{\infty} \mathrm{Ai}(z)\,dz, \quad Q = i^{1/3}k^{1/3}|k|$$

Taking into account that

$$f_F = -\frac{2}{k^2}\left(1 - \frac{a}{a-b}e^{-ibk} + \frac{b}{a-b}e^{-iak}\right)$$

is the Fourier transform of the function f given by (1.4), we have /6-9/

$$\bar{p} = -\omega_0 |k| f_F(k)\,\Phi(\Omega)[(\omega^2 + \omega_0^2)F(\Omega, k)]^{-1} \tag{2.3}$$

Let us clarify how the pressure changes along the boundary layer. Calculation of the perturbed velocity vector components, although more complex in technical respects, does not encounter any new problems, in principle, during the solution.

Inversion of the formula for $\bar{p}$ requires a knowledge of the structure of both the complex planes ω and k. If we start with the calculation of the inverse Laplace transform, then k will play the part of a real (negative or positive) parameter. Under the condition, there are no other singularities in the ω plane besides the denumerable set of poles of the function-transform. The second plane in which the subsequent examination of the inverse Fourier transform will proceed, appears much more complicated. Indeed, the passage over to the variable z by using relationship (2.1) and the extraction of a single-valued branch for the function $k^{1/3}$ requires, firstly, drawing a slit along the positive imaginary half-axis from the origin to infinity. Furthermore, the quantity $F(\Omega, k)$ in the denominator of (2.3) for $\bar{p}$ constrains the non-analytic function $|k|$. On being equated to zero it yields the dispersion relation /6-9/

$$\Phi(\Omega) = Q(k) \tag{2.4}$$

that connects the frequency to the free-oscillation wave number. Finally, a denumerable number of branch points is located in the complex k plane, and their appearance is due to the possibility of interaction of the dispersion curves and they must be taken into account in the inverse Fourier transform during deformation of the path of integration. However, it is essential that none of the branch points under consideration be incident on the real axis.

Let $\Omega_m(k)$ be the m-th root of Eq.(2.4) and $\omega_m(k)$ its corresponding dispersion curve, where $m = 1, 2, \ldots$. From the definition (2.2) of the functions F and Φ the following differential connection results

$$\frac{d\,\mathrm{Ai}[\Omega_m(k)]}{d\Omega}\,\frac{d\Phi[\Omega_m(k)]}{d\Omega} = \Phi[\Omega_m(k)]\frac{\partial H[\Omega_m(k), k]}{\partial\Omega} \tag{2.5}$$

$$H = F(\Omega, k)\,I(\Omega) = d\mathrm{Ai}(\Omega)/dz - i^{1/3}k^{1/3}|k|\,I(\Omega) \tag{2.6}$$

For real k the real part of $\omega_1(k)$ can take on both negative and positive values. All the remaining dispersion curves $\omega_m(k)$ lie entirely in the left ω half-plane. The equality $\mathrm{Re}\,\omega_1(k) = 0$ fixes the critical frequency $\omega_* = 2.298$ and the wave number $k_* = 1.0005$, that characterize the neutral oscillations.

Making use of the fact that for real k all singularities of $\bar{p}$ in the ω plane reduce to a denumerable set of poles, we expand the inverse Laplace transform in a series in the residues of the integrand. For $t \gg 1$ there will be two main terms of the series, and the application of the Laplace lemma to the sum of the remaining terms will result in an estimate $O(t^{-6})$ uniformly in x /2/. Further analysis is based on neglecting the sum mentioned.

The simplification performed enables us to write the inverse Fourier transform as /2, 9/

$$p' = \frac{1}{\pi}\mathrm{Re}\,[I_1(x)\exp(i\omega_0 t) + I_2(t, x)] \tag{2.7}$$

$$I_1 = \frac{i}{2}\int_{-\infty}^{\infty} |k| f_F(k)\frac{d\,\mathrm{Ai}[\Omega_0(k)]}{d\Omega}e^{ikx}\frac{1}{H[\Omega_0(k), k]}\,dk$$

$$I_2 = -i^{1/3}\omega_0 \int_0^\infty k^{1/3} f_F(k) \frac{d\,\mathrm{Ai}\,[\Omega_1(k)]}{d\Omega} \exp(\omega_1(k)\,t + ikx) \times$$
$$\{[\omega_1^2(k) + \omega_0^2]\,\partial H[\Omega_1(k), k]/\partial\Omega\}^{-1}\,dk$$

if we set $\Omega_0 = i^{1/3}\omega_0 k^{-2/3}$ and return to the differential connection (2.5) in combination with the definition (2.6) of the function H.

The first component in (2.7) for p' yields the fluctuation of the excess pressure near the vibrator, which, according to /8/, damp out as $O(x^{-2})$ for all frequencies except the critical one. Since the fundamental aim is clarification of the perturbation mode in the limit when not only $t \gg 1$ but also $x \gg 1$, this component can generally be omitted because of smallness, but to keep the picture complete, the correction it specified was taken into account in constructing some of the graphs presented below that refer to moderate times and distances from the source.

3. **The complex Ω and k planes.** For the subcritical frequencies $\omega_0 < \omega_*$ the integral I_2 yields a contribution $O(t^{-6})$ to the pressure fluctuations in the domain $x < V_b t$, where V_b is a constant. For vibrator operation at the post-critical frequencies $\omega_0 > \omega_*$ the same integral describes a Tollmien-Schlichting wave with exponentially increasing amplitude of the oscillations in the domain mentioned. The results that were obtained in /2/ are the foundation for the postulate put forward in /1/ that governs the structure of the perturbations as the frequency of the harmonic oscillator passes through the critical value.

We evaluate the constant V_b and study what occurs in the domain $x > V_b(t)$ for both the sub- and the post-critical frequencies. After (2.6) has been differentiated the integral I_2 takes the form

$$I_2 = -i^{1/3}\omega_0 \int_0^\infty \chi(k; \omega_0) \exp(t\varphi(k; V))\,dk \tag{3.1}$$
$$\chi = k^{1/3} f_F(k)\,d\mathrm{Ai}\,[\Omega_1(k)]/d\Omega \quad \{[\omega_1^2(k) + \omega_0^2]\,[\omega_1(k) + ik^2]\,\mathrm{Ai}\,[\Omega_1(k)]\}^{-1}$$
$$\varphi(k; V) = \omega_1(k) + iVk; \quad V = x/t \tag{3.2}$$

The asymptotic expansion of ω_1 as $|k| \to \infty$ and $-\pi/8 < \arg k < \pi/2$ states

$$\omega_1 = -ik^2 + \sqrt{2}\,(1 - i)/2 + \ldots \tag{3.3}$$

from which for real positive k to a first approximation $\mathrm{Re}\,\varphi = \sqrt{2}/2$. In this connection, integration along the real axis in the first of the formulas in (3.1) is difficult since the convergence of I_2 is achieved just because of the function χ which decreases as $|k|^{-3}$ as $|k| \to \infty$. For large values of $|k|$ the path of integration should be deformed in such a way that it would go into the fourth quadrant of the plane k, for examples parallel to, but below the real axis. The deformation mentioned ensures that the integrand in I_2 tends to zero exponentially, whereupon in this case the principal term $\mathrm{Re}\,\varphi = 2\,\mathrm{Re}\,k \cdot \mathrm{Im}\,k$ and $\mathrm{Im}\,k < 0$. It is understood that by deforming the initial path of integration, the poles and branch points of the integrand, which are incident in the domain bounded by the new contour, must be taken into account.

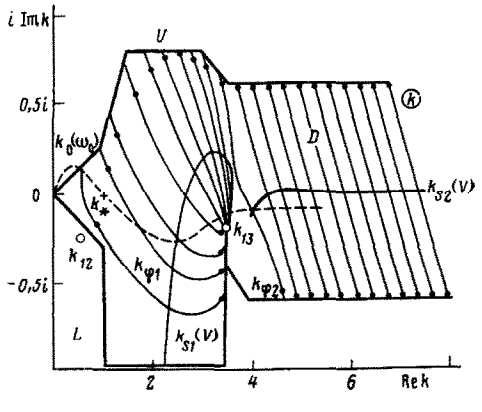

Fig.1

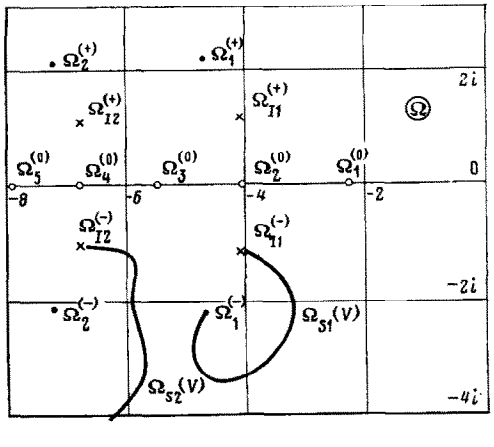

Fig.2

The location of the first singularity, the simple pole $\omega_1(k) = -i\omega_0$, depends on the vibrator

frequency ω_0, its trajectory k_0 is shown in Fig.1, where ω_0 grows along the curve as one moves away from the origin. For $\omega_0 = \omega_*$ it intersects the real axis ay the point $k = k_*$. When $\omega_0 \to \infty$ the shape of the trajectory is built up by using the asymptotic expansion (3.3) for ω_1.

The existence of other zeros of the denominator of the function χ from the integrand in I_2 is due to the disappearance of the product $\mathrm{Ai}[\Omega_1(k)][\omega_1(k) + ik^2]$. The roots of the equation obtained in this manner are double roots of the dispersion relation (2.4). In the complex Ω plane they are displayed by the common points Ω_{mn} of its simple roots $\Omega_m(k)$ and $\Omega_n(k)$. Indeed, let Φ and $d\Phi/d\Omega$ remain bounded as $\Omega \to \Omega_{mn}$; then together with the dispersion relation itself the double roots should satisfy the additional equality

$$d\Phi/d\Omega = \mathrm{Ai}(\Omega)[\Omega + \Phi(\Omega)]I^{-1}(\Omega) = 0 \tag{3.4}$$

from which the assertion formulated above results. It follows from (3.4) that under the assumption made the points Ω_{mn} are generated by zeros of one of the functions $\mathrm{Ai}(\Omega)$ or $\psi = \Omega + \Phi(\Omega)$. As is well-known, the zeros $\Omega_j^{(0)}$ of the Airey functions lie on the real negative semi-axis (they are denoted by open circles in Fig.2). All the pairs of complex-conjugate zeros $\Omega_j^{(-)}$ and $\Omega_j^{(+)}$ of the function ψ are in the left half-plane and denoted by the dark points.

We will examine the nature of the singularities that occur when the integral I passes through zero from the denominator of the expressions for both the function Φ and its derivative $d\Phi/d\Omega$. The corresponding points $\Omega_{jj}^{(-)}$ and $\Omega_{jj}^{(+)}$ are complex-conjugates and are also in the left half-plane (they are denoted by crosses in Fig.2). The expansion

$$\Omega - \Omega_{jj}^{(\mp)} = -i^{-1/3}\frac{d\,\mathrm{Ai}[\Omega_{jj}^{\mp}]}{d\Omega}\frac{1}{\mathrm{Ai}[\Omega_{jj}^{(\mp)}]k^{1/3}} + \ldots |k| \to \infty$$

is valid in their neighbourhood.

Since $k^{-1/3}$ is a single-valued function int the plane with the slit along the imaginary positive half-axis from the origin to infinity, the zeros of the integral I do not yield new branch points for the roots of the dispersion relation. In all the cases to be discussed below, j runs through the values $1, 2, \ldots$.

The points under consideration in the Ω plane generate singular points k_{mn} in the k plane, out of which $k_{12} = k_1^{(0)} = 0.590 - 0.244i$ and $k_{13} = k_1^{(-)} = 3.444 - 0.207i$ must be taken into account in I_2 during deformation of the path of integration. These are determined by the equalities $\mathrm{Ai}[\Omega_1(k)] = 0$ and $\omega_1(k) + ik^2 = 0$, i.e. are points where the first root $\Omega_1(k)$ of the dispersion relation takes equal values with the second $\Omega_2(k)$ and third $\Omega_3(k)$ roots. It hence follows that the singular points k_{12} and k_{13} are not only zeros of the denominator of χ but also branch points of the function $\omega_1(k)$ from the integrand in I_2.

4. Selection of the contour of integration. Taking account of the remarks made, we deform the path of integration in I_2 along the real positive half-axis into a new contour, denoted by L in Fig.1, in such a way as to remain at the side of the point k_{12}. The deformed contour encirles the singular point k_{13}, approaches and leaves it along the edges of the slit drawn from this point. For $\mathrm{Re}\,k \geqslant 3.8$, a line located below the trajectory k_0 parallel to the real axis is L. The spacing between L and the real axis will be selected later. When $|k| \to \infty$ the advantages of integrating along L are obvious. The desirability of going over to the new contour for small and moderate values of $|k|$ requires discussion. The solution of this question depends on what are the values of the time t and the constant V in (3.2) for the exponent $t\varphi$. In laboratory experiments, growth of the vortex spot amplitude is replaced by a non-linear development process at small distances from the source at the end of a finite interval t after the triggering /10/. In order to be able to compare the theoretical results with test data it is not enough to examine just the limit case $t \gg 1$.

We rewrite the integral I_2 as follows

$$I_2 = i^{-1/3}\omega_0\{\int_L \chi(k;\omega_0)\exp(t\varphi(k;V))\,dk - \tag{4.1}$$
$$2\pi i\theta(\omega_0 - \omega_*)\,\mathrm{res}\,[\chi(k;\omega_0)\exp(t\varphi(k;V))]_{k=k_1(\omega_0)}\}$$

where θ is the Heaviside unit function. For $\omega_0 > \omega_*$ the second term on the right hand side of (4.1) is a Tollmien-Schlichting wave. As calculations showed, the firt term tends to zero for $V \leqslant 2.4$ if $t \to \infty$. It therefore follows that the constant $V_b = 2.4$ and the use of L as the path of integration is justified in the range of V mentioned. Constraining the time interval by the inequalities $3 \leqslant t \leqslant 10$, the range of apllication of L can be extended to $V \leqslant 3.5$. However, as V increases to 4.0 the integrand in the second term on the right-hand side of (4.1) rapidly becomes oscillatory, which requires the introduction of a very shallow step of integration. The integral itself increases radically: for $t = 10$ it is of the order of 10^4. Despite the rapid convergence of this integral as $|k| \to \infty$, it becomes difficult to ensure high accuracy of the calculations if $V > 3.5$. It is clear that further deformation of L into a new or even a system of contours is necessary.

Their search relies on the idea underlying the saddle-point method. However, for comparitively small times $3 \leqslant t \leqslant 10$ the saddle-point method in its classical formulation yields a substantial error in evaluating the first term on the right side of (4.1). For any fixed V the coordinates of the saddle point satisfy the equation

$$d\varphi/dk = d\omega_1/dk + iV = 0 \tag{4.2}$$

whose solution is denoted by $k_s = k_s(V)$. As calculations carried out on a computer showed, the function $k_s(V)$ has two branches $k_{s1}(V)$ and $k_{s2}(V)$, shown in Fig.1. The former is associated with the singular point k_{13} and the expansion

$$(\Omega_1 - \Omega_{13})^3 = \frac{8}{3} i^{3/2} k_{13}^{3/2} [d^2\Phi(\Omega_{13})/d\Omega^2]^{-1} (k - k_{13}) + \ldots$$
$$d^2\Phi(\Omega_{13})/d\Omega^2 = -\Omega_{13}\mathrm{Ai}(\Omega_{13}) [d\mathrm{Ai}(\Omega_{13})/d\Omega]^{-1}, \quad \Omega_{13} = -i^{1/3} k_{13}^{4/3}$$

is valid in its neighbourhood, while the latter enables us to find the derivative

$$d\omega_1/dk = {}^2/_3 i^{3/2} k^{-3/2} \Omega_1(k) + i^{3/2} k^{3/2} d\Omega_1/dk$$

from (4.2) as $k \to k_{13}$. The curve $k_{s1}(V)$ starts from the infinitely remote point of the k plane for $V = 0$, which corresponds to the point $\Omega_{11}^{(-)} = -4.107 - i1.144$ in the Ω plane. It then intersects the contour L, envelops the point k_{13} from above and is based on it in the limit as $V \to \infty$. The second branch $k_{s2}(V)$ starts from the infinitely remote point of the k plane for $V = 0$, which corresponds to $\Omega_{12}^{(-)} = -6.798 - i\,1.035$, emerges on the first sheet of the Riemann surface from under the slit drawn through k_{13}, intersects the real axis and departs along the real axis for the infinitely remote point of the k plane corresponding to the infinitely remote point of the Ω plane as $V \to \infty$. Trajectories of the saddle points generated by the branches $k_{s1}(V)$ and $k_{s2}(V)$

$$\Omega = \Omega_{s1}(V) = \omega_1(k_{s1}(V)) [ik_{s1}(V)]^{-3/2}$$
$$\Omega = \Omega_{s2}(V) = \omega_1(k_{s2}(V)) [ik_{s2}(V)]^{-3/2}$$

in the Ω plane are presented in Fig.2.

The nature of the change in $\mathrm{Re}\,\varphi(k_{s1}, V)$ and $\mathrm{Re}\,\varphi(k_{s2}, V)$ along the curves $k_{s1}(V)$ and $k_{s2}(V)$ can be elucidated from Fig.3, where they are marked with the numbers *1* and *2*, respectively.

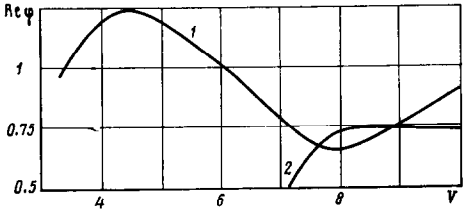

Fig.3

We skip through every point of the curve $k_{s1}(V)$ with a fixed value V to the line $k_{\varphi 1}$ carrying the constant value

$$\mathrm{Im}\,\varphi(k; V) = \mathrm{Im}\,\varphi[k_{s1}(V); V]$$

On this line we note those points where $\mathrm{Re}\,\varphi(k_{\varphi 1}; V) = 0$ by dark circles. As V changes these points move forming two branches, one of which is located almost entirely in the upper k half-plane, while the other passes near the edges of the slit drawn through k_{13}. Two circumstances play a substantial role: the first branch intersects the contour L for $V \approx 3.2$, and bending of the second branch is accompanied by its displacement under the slit for $V \approx 7.4$.

We return to the domain D in Fig.1, which is bounded from above by the contour U and from below by the contour L. The former is selected so that for $3.2 < V < 7.4$ both branches of the curve formed by the dark points do not leave D. We connect points of the contours U and L by a system of lines $k_{\varphi 1}$. In conformity with Fig.3, $\mathrm{Re}\,\varphi(k_{\varphi 1}, V) \geqslant 0$ on a segment of each such line cut off by the two branches of the curve of dark points, where the maximum is reached at the saddle point.

The range in which the second term from the right side of (4.1) is obtained by an integration path along L can be constructed now to $0 \leqslant V \leqslant 3.2$ if the comparatively small times $3 \leqslant t \leqslant 10$ are considered. For each V from the interval $3.2 \leqslant V \leqslant 7.4$ its contour of integration consisting of three parts should be chosen. The section of U from the origin to the point of intersection with the line $k_{\varphi 1}$ carrying prescribed values of V and $\mathrm{Im}\,\varphi(k; V)$ forms the first; the second part agrees with the segment $k_{\varphi 1}$ from D; and the section of L from the point of intersection with the line $k_{\varphi 1}$ to infinity yields the third. Along the first and third parts of the new contour $\mathrm{Re}\,\varphi(k; V) \leqslant 0$, which ensures smallness of the contributions due to these parts in I_2. Along the second part $\mathrm{Im}\,\varphi(k; V) = \mathrm{const}$, the rapidly oscillating term $\exp[it\,\mathrm{Im}\,\varphi(k; V)]$ is taken outside the integral sign while the rest of the integrand varies smoothly. Consequently, a comparatively coarse spacing can be used for integration along $k_{\varphi 1}$. An analogous contour deformation is the crux of the saddle-point method, but the integral desired in it is evaluated over a small section in the immediate vicinity of the saddle point under the assumption that $t \to \infty$. The fuller analysis elucidated above about how the contour of integration should be transformed for the computation of I_2 by means of (4.1), enables us to consider the moderate values $3 \leqslant t \leqslant 10$.

To evaluate the magnitude of I_2 by means of (4.1) for $7.4 \leqslant V < \infty$ it would be natural

to construct a system of lines $k_{\varphi 2}$ which would pass through points of the curve k_{s_2} with fixed V and carry the constant values

$$\operatorname{Im} \varphi (k;\ V) = \operatorname{Im} \varphi [k_{s_2}(V);\ V]$$

However, it is impossible to realize this program completely because a line $k_{\varphi 2}$ that connects both geometric sites k_{s1} and k_{s_2} of the saddle points exists for a certain V from the interval $7.93 < V < 7.95$ It is determined by V from the equation

$$\operatorname{Im} \varphi [k_{s1}(V),\ V] = \operatorname{Im} \varphi [k_{s_2}(V);\ V]$$

and is a separatrix: the lines $k_{\varphi 2}$ located below it depart to the second sheet of the Riemann surface under the slit drawn through k_{13}, and only lines $k_{\varphi 1}$ lying above it connect the contour U to the contour L, forming a new path of integration. The topology of the curves in the k plane for the interval of V under consideration is seen in Fig.4.

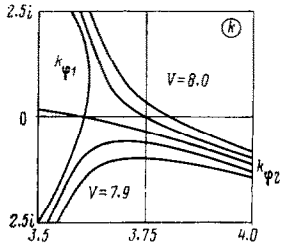

Fig.4

Since the lines $k_{\varphi 2}$ for $7.4 \leqslant V \leqslant 7.95$ cannot be used to evaluate the integral term from the right-hand side of (4.1), we compile a path of integration from sections of the contours U and L by connecting them as before by using the segments $k_{\varphi 1}$. At the point of intersection of $k_{\varphi 1}$ with L we have $\operatorname{Re} \varphi (k_{\varphi 1};\ V) > 0$, hence, the contributions to I_2 due to integration over $k_{\varphi 1}$ and L become comparable in magnitude. Understandably, elevated requirements should be imposed on the method of approximate calculations to conserve their accuracy (as t grows these requirements are naturally weakened).

For $7\ 95 \leqslant V < \infty$ each of the lines $k_{\varphi 2}$ not only connects U and L but also possesses two points where $\operatorname{Re} \varphi (k_{\varphi 2};\ V) = 0$. The curves drawn through these points, denoted by the dark circles in Fig.1, from branches, one of which is in the upper half-plane and the other in the lower. The horizontal lines going off to infinity, by which the contours U and L are terminated, are placed at such a distance from the real axis that the curves drawn through the dark circles would lie entirely in the domain D.

In order to extract all the advantages of the saddle point method for evaluating the integral term from the right-hand side of (4.1) in the last $7.95 \leqslant V < \infty$ and the moderate $3 \leqslant t \leqslant 10$ ranges, integration should start along the contour U up to the intersection with the line $k_{\varphi 2}$ with given V, then continued to $k_{\varphi 2}$ carrying the constant value $\operatorname{Im} \varphi (k;\ V)$, and terminate along the contour L from the point of its intersection with the line $k_{\varphi 2}$ to infinity. The inequality $\operatorname{Re} \varphi (k;\ V) < 0$, which is valid at each point on the first and third sections of the path under consideration, ensures the smallness of the contributions from the corresponding integrals to I_2. Actually, only the contribution collected during integration along the segment $k_{\varphi 2}$ with saddle point approximately at its middle is essential for calculating the quantity desired.

5. Results of calculations. As mentioned above, in laboratory experiments the growth of the vortex spot amplitude is replaced fairly rapidly by the extremely non-linear process of their development /10/. Consequently, the times in the computations were selected to be moderate from the range $3 \leqslant t \leqslant 10$. Because of the differences in the magnitudes of the Reynolds numbers R used in the theory and achievable in tests, the quantitative comparison of any of these results turns out to be all but impossible: by the assumption on which the present analysis is based $R \to \infty$, while comparatively low local values of R have been realized in a plate in a low-turbulence tube up to now. The graphs presented above enables us, however, to trace what qualitative regularities are inherent in wave packets during their formation and propagation to distances observable in experiments. Understandably, the illustrative material contains only part of the data obtained, whose derivation with a computer was realized with an interval $\Delta t = 1$.

The calculation process was organized as follows. For an approximate determination of the second term on the right-hand side of (4.1), the contour L is used as the path of integration if $0.1 < V < 3.2$. Composite paths of integration were used when $3.2 \leqslant V \leqslant 13$, where besides the segments of the contours U and L they included the lines $k_{\varphi 1}$ for $3.2 \leqslant V < 8$ and the lines $k_{\varphi 2}$ for $8 \leqslant V \leqslant 13$. The step $\Delta V = 0.1$ ensured the necessary accuracy of the calculations in all cases, although the integrals over $k_{\varphi 1}$ and L in the interval $7.4 \leqslant V \leqslant 7.9$ were comparable in magnitude.

The lengths of the contours U and L are fixed by their intersections with the lines $k_{\varphi 2}$ drawn through the curve k_{s_2} under the condition $V = 13$. The analysis was cut off here since the amplitude of the perturbations became quite small. Along U and L the functions $\omega_1 (k)$ and $\chi (k;\ \omega_0)$ were computed with a fairly shallow step in k for any given value of V. Thus, 600 points were on U while the quantity reached 1500 on L because of the need to traverse the edges of the slit drawn through k_{13}. Both systems of lines $k_{\varphi 1}$ and $k_{\varphi 2}$ are aligned with a step $\Delta V = 0.1$ and of the order of 150 points were utilized along each such line to compute

$\omega_1(k)$ and $\chi(k; \omega_0)$.

It is still necessary to select the vibrator parameters: we set $a = 2$, $b = 1$ in the extension of /2, 8/. As regards the frequency of its oscillations ω_0, we then consider three cases as typical: $\omega_0 = 2.0; 5.0; 7.3$. The pressure distribution along the boundary layer for the first of these cases is shown in Fig.5 for the times $t = 3; 6; 10$ (because of lack of space, we will comment only briefly on results referring to the other two cases). The critical frequency $\omega_* = 2.298$ lies between the first two frequencies $\omega_0 = 2.0$ and $\omega_0 = 5.0$ of vibrator operation. The third value $\omega_0 = 7.3$ corresponds to free selfexciting oscillations with a maximal increment in the amplitude growth along the longitudinal coordinate. For low times and all ω_0 the correction given in (2.7) for p' by the integral I_1 should be taken into account. The method for evaluating it is described in /8/.

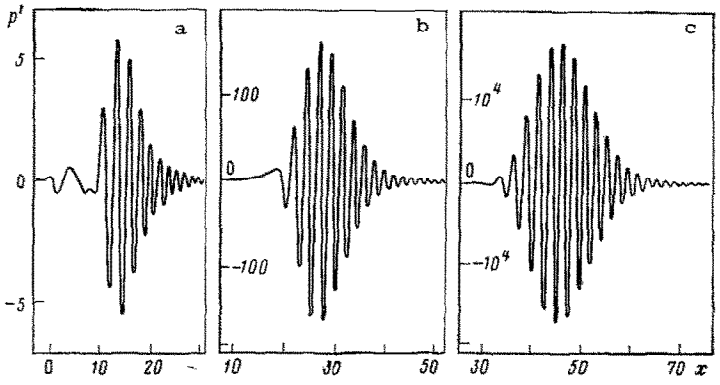

Fig.5

The time $t = 3$ can be considered transitional for all regimes: at the end of such a small time interval after triggering the vibrator, the perturbations in its neighbourhood are, albeit considerably less, but still comparable in order of magnitude with the fluctuations at the centre of the vortex spot. The invalid nature of the wave packet formation is manifested most clearly at the subcritical frequencies (Fig.5a) while the process is more complete for post-critical frequencies.

If $\omega_0 = 2.0$, then the vortex spot is separated from the source to the time $t = 6$ (Fig. 5b), and takes a fully completed form at $t = 10$ (Fig.5c). It is not subjected to the action of the source of oscillations that damp out quite rapidly with distance during its further motion. The perturbation field in the forward part of the spot and its centre is practically unchanged at all the subscritical frequencies, but the rear part changes slightly depending on the magnitude of ω_0. From this viewpoint triggering of a harmonic oscillator with a subcritical frequency is barely different from the impulsive connection being performed in experiments /10/.

As computations show, at post-critical frequencies the rear part of the vortex spot at the time $t = 6$ is continuously referred to the Tollmien-Schlichting wave being started at the vibrator with a wave number corresponding to a given ω_0 which is found from solving the dispersion relation (3.4). The fluctuations at the centre and forward part of the wave packets are similar in nature to that already discussed in Fig.5b the fact that they have a large amplitude in order of magnitude. Here the perturbation field is determined principally by the internal properties of the boundary layer with selfinduced pressure, but, according to (1.6), the vertical component of the velocity vector on the membrane surface is proportional to ω_0 at the initial time, whereupon the span of the oscillations changes as the frequency of the forcing force increases.

The pattern just described for the vortex spots being formed at post-critical frequencies is conserved at the time $t = 10$. Further evolution of the wave packets causes the impression of their separation from the source,which is deceptive. The fact is that the amplitude of the fluctuations in the Tollmien-Schlichting wave grows exponentially downstream of the vibrator. For large times the span of the oscillations in its neighbourhood is many times less than in the intermediate domain where the Tollmien-Schlichting wave is connected with the rear part of the vortex spot. For $t = 10$ the domain between the source and the spot turns out to be perturbation-free although this estimate is smoothed out somewhat for the frequency $\omega_0 = 7.3$, that corresponds to free selfexciting oscillations with maximum growth of the amplitude along the longitudinal coordinate. We note that the excess pressure at the centre of the vortex spot does not reach the value that it would for continuous continuation of the Tollmein-Schlichting wave in the designated domain.

For both subcritical and post-critical frequencies the vortex spot broadens as it

propagates downstream. According to /11/, extrema $\mathrm{Re}\,\omega_1(k)$ hold at the points $k_1^* = 0.523$, $k_2^* = 2.716$, $k_3^* = 3.616$, $k_4^* = 4.346$, located on the real axis in the k plane, where positive maxima are realized in the second and fourth. It hence follows that the vortex spot under consideration or the wave packet consists of two subpackets joined into one. The maximum at the point $k = k_2^*$ is quite definite, the amplitude of its corresponding subpacket possesses the greatest growth increment in time. This is the centre of the vortex spot propagating at the group velocity $V_2^* = -d\,\mathrm{Im}\,\omega_1(k_2^*)/dk = 4.49$, here the span of the oscillations reaches the maximum value. The local maximum at $k = k_4^*$ is hardly noticed compared with the values of $\mathrm{Re}\,\omega_1(k)$ at the adjacent points on the real axis, its corresponding wave subpacket whose group velocity is $V_4^* = -d\,\mathrm{Im}\,\omega_1(k_4^*)/dk = 8.63$, is not extracted by anything in the forward part of the spot. The boundary between both wave subpackets is determined by the local minimum $\mathrm{Re}\,\varphi(k_{s1}, V) = \mathrm{Re}\,\varphi(k_{s2}, V)$, and the velocity of its displacement is $V_3 = -d\,\mathrm{Im}\,\omega_1(k_3^*)/dk = 7.64$. As before, this extremum is denoted weakly, consequently, the boundary between the subpackets is not distinguishable in Fig.5 where the vortex spot appears as a single formation in the later stages $(t > 3)$.

The wave number $k = k_2^*$ determines the free selfexciting oscillations with the greatest amplitude growth in time. Their frequency ω_2^* has the parameters $\mathrm{Re}\,\omega_2^* = 1.24$ and $\mathrm{Im}\,\omega_2^* = -8.16$. The dependence of the excess pressure at the centre of the vortex spot on the vibrator operating frequency ω_0 was noted above. For $t \gg 1$ and $x \gg 1$ this dependence can be found by using the saddle point method, where the line $k_{\varphi 1}$ passing through the point of the curve k_{s1} with $V = V^*_2$ should be utilized by deforming the path of integration for calculating the second term on the right-hand side of (4.1). The latter obviously agrees with the point $k = k_2^*$. Hence, the magnitude of the perturbations at the centre of the spot is obtained proportional to the coefficient $q = \omega_0 |\,\omega_1^2(k_2^*) + \omega_0^2\,|^{-1}$ that reaches a maximum for $\omega_0 = |\,\omega_1(k_2^*)\,| = |\,\omega_2^*\,| = 8.25$. The change in q as ω_0 increases is shown in Fig.6.

In conclusion, we establish the nature of the perturbations in a long wave tongue extended in front. Its existence results from the fact that $\mathrm{Re}\,\omega_1(k) \to \mathrm{const} = \sqrt{2}/2$ as $k \to \infty$ along the real axis. The excess pressure in this domain is small, the Kelvin method of stationary phase, on the basis of the assumption $V \gg 1$, was used to compute it in /9/. The latter is in agreement with the calculation procedures described above which were cut off at the point of intersection of the contour L with the line $k_{\varphi 2}$ carrying the value $V = 13$. Repeating the reasoning in /9/, we have

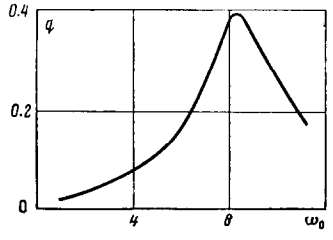

Fig.6

$$p' = \mathrm{Re}\left\{2^4\pi^{-1/2}\omega_0\left[1 - \frac{a}{a-b}\exp(-ixb/(2t)) + \frac{b}{a-b}\exp(-ixa/(2t))\right] t^{1/2}x^{-3}\exp(t/\sqrt{2})\times \exp(i(x^2/t - 2\sqrt{2}t + \pi)/4)\right\} \quad (5.1)$$

To conclusions of a qualitative aspect result from (5.1). Firstly, the structure of the perturbations in the domain under consideration depends on the initial stage of triggering the vibrator being distinguished from that obtained during impulsive blowing of a jet into the boundary layer through a hole cut in the streamlined plate. Secondly, superposition of the waves results in origination of fine-scale oscillations governed by the ratio x^2/t in the exponent, even in the linear stage of the process of interaction between different modes. However, the amplitude of these oscillations is extremely small. They were not determined in the experiments /10/.* (*See also: Gilev, V.M. and Kozlov, V.V., A method of creating two- and three-dimensional wave packets in the boundary layer. Preprint. Inst. Teoret. Prikl. Mekhaniki Sibirsk. Otdel. Akad. Nauk SSSR, No.2, Novosibirsk, 1980).

The above analysis is based on the theory of free boundary layer interaction, which correctly describes the asymptotic form of the lower branch of the neutral stability curve. As has recently been shown /12, 13/, this theory applies to a study of the selfexciting oscillations in almost the whole domain enclosed between both branches of the neutral loop (the exception is the nearest neighbourhood of the upper branch). Taking account of the latter can be expressed just in a more accurate computation of the amplitude perturbations which are vanishingly small compared with the span of the fluctuations at the centre of the vortex spot.

The ratio between the free selfexciting oscillations with maximum amplitude growth increment in space and the neutral frequency is approximately 3.17, which is in satisfactory agreement with the analogous quantity cited in /14/ as a result of numerical integration of the Orr-Sommerfeld equation for moderate values of the Reynolds numbers.

REFERENCES

1. BOGDANOVA E.V. and RYZHOV O.S., On perturbations generated by oscillators in a viscous fluid flow at post-critical frequencies. Prikl. Mekh. Tekh. Fiz., 4, 1982.
2. TERENT'EV E.D., The linear problem of a vibrator performing harmonic oscillations at beyond-critical frequencies in a subsonic boundary later, PMM, 48, 2, 1984.
3. NEILAND V.YA., Asymptotic problems of the theory of viscous supersonic flows. Trudy, TsAGI, 1529, 1974.
4. STEWARTSON K., Multistructured boundary layers on flat plates and related bodies. Advances in Applied Mechanics, 14, Academic Press, N.Y., 1974.
5. RUBAN A.I. and SYCHEV V.V., Asymptotic theory of laminar boundary layer separation in an incompressible fluid, Uspekhi Mekhaniki, 2, 4, 1979.
6. RYZHOV O.S. and TERENT'EV E.D., On the non-stationary boundary layer with selfinduced pressure, PMM, 41, 6, 1977.
7. RYZHOV O.S. and ZHUK V.I., Internal waves in the boundary layer with selfinduced pressure, J. Mec., 19, 3, 1980.
8. TERENT'EV E.D., The linear problem of a vibrator in a subsonic boundary layer, PMM, 45, 6, 1981.
9. RYZHOV O.S. and TERENT'EV E.D., On certain properties of vortex spots in the boundary layer on a plate. Dokl. Akad. Nauk SSSR, 276, 3, 1984.
10. GASTER M. and GRANT I., An experimental investigation of the formation and development of a wave packet in a laminar boundary layer. Proc. Roy. Soc. A, 374, 1649, 1975.
11. ZHUK V.I. and RYZHOV O.S., Free interaction and stability of the boundary layer in an incompressible fluid, Dokl. Akad. Nauk SSSR, 253, 6, 1980.
12. ZHUK V.I. and RYZHOV O.S., On the asymptotic of solutions of the Orr-Sommerfeld equation that yield unstable oscillations for large values of the Reynolds number, Dokl. Akad. Nauk SSSR, 268, 6, 1983.
13. ZHUK V.I., On the asymptotic form of solutions of the Orr-Sommerfeld equations in domains adjoining two branches of the neutral curve, Izv. Akad. Nauk SSSR, Mekhan. Zhidk. Gaza, 4, 1984.
14. LIN C.C., Theory of Hydrodynamic Stability, IIL, Moscow, 1958.

Translated by M.D.F.

PMM U.S.S.R.,Vol.50,No.6,pp.762-769,1986
Printed in Great Britain

0021-8928/86 $10.00+0.00

REMOTE STATIONARY WAVE FIELD GENERATED BY LOCAL PERTURBING SOURCES IN A FLOW OF STRATIFIED FLUID*

V.F. SANNIKOV

A linear formulation is used to study the problem of stationary waves formed in a uniform flow of an inviscid incompressible vertically stratified fluid past a point source or a mass dipole. Formulas are derived representing the characteristics of the wave field in the form of the sum of single integrals. A method is developed for constructing complete asymptotic expansions of the integrals obtained for large distances from the wave generator, including uniform expansions near the leading fronts of the separate modes. Approximate solutions of the problem in question exist (/1-4/ et al.). The behaviour of the characteristics of the wave field near the leading fronts of internal waves was studied in /5, 6/. In the case of a deep liquid the asymptotic form uniform in the neighbourhood of the leading fronts is expressed in terms of Fresnel integrals /5/, and in the case of a liquid of finite depth by Airy functions /6/. Examples of the exact solution of the problem are given in /7/.

*Prikl.Matem.Mekhan.,50,6,987-995,1986